

Erratum: "Detecting Reconnection Events in Kinetic Vlasov Hybrid Simulations Using Clustering Techniques" (2021, ApJ, 908, 107)

Manuela Sisti, Francesco Finelli, Giorgio Pedrazzi, Matteo Faganello, Francesco Califano, Francesca Delli Ponti

▶ **To cite this version:**

Manuela Sisti, Francesco Finelli, Giorgio Pedrazzi, Matteo Faganello, Francesco Califano, et al.. Erratum: "Detecting Reconnection Events in Kinetic Vlasov Hybrid Simulations Using Clustering Techniques" (2021, ApJ, 908, 107). The Astrophysical Journal, 2021, 917 (1), pp.51. 10.3847/1538-4357/ac1747 . hal-03667194

HAL Id: hal-03667194
https://amu.hal.science/hal-03667194

Submitted on 13 May 2022

HAL is a multi-disciplinary open access archive for the deposit and dissemination of scientific research documents, whether they are published or not. The documents may come from teaching and research institutions in France or abroad, or from public or private research centers.

L'archive ouverte pluridisciplinaire **HAL**, est destinée au dépôt et à la diffusion de documents scientifiques de niveau recherche, publiés ou non, émanant des établissements d'enseignement et de recherche français ou étrangers, des laboratoires publics ou privés.



Distributed under a Creative Commons Attribution 4.0 International License

The Astrophysical Journal, 917:51 (3pp), 2021 August 10 https://doi.org/10.3847/1538-4357/ac1747
© 2021. The American Astronomical Society. All rights reserved.

Erratum: "Detecting Reconnection Events in Kinetic Vlasov Hybrid Simulations Using Clustering Techniques" (2021, ApJ, 908, 107)

Manuela Sisti[1,2], Francesco Finelli[2], Giorgio Pedrazzi[3], Matteo Faganello[1], Francesco Califano[2], and Francesca Delli Ponti[3]
[1] Aix-Marseille University, CNRS, PIIM UMR F-7345, Marseille, EU, France; manuela.sisti@univ-amu.fr
[2] Dipartimento di Fisica, Università di Pisa, Italy
[3] HPC Department, Cineca, Bologna, Italy
Received 2021 July 19; revised 2021 July 21; published 2021 August 16

While the physical picture that emerges is correct, we regret the presence of a bug in the code for the estimation of the aspect ratio of the candidate structures found. In particular, a factor $\sqrt{2}$ was inadvertently set in the estimation of the thickness, leading to an underestimation of the AR by a factor $1/\sqrt{2}$. The revised Tables 3, 4, and 5 with the corrected values of AR are reported in the following, together with the corrected Figure 6. As anticipated the physical picture is the same, with only a slightly different value of the "optimal" AR threshold. The new "optimal" AR threshold is $\simeq 26$. In the published article we shared the link to our codes, which will become a tool, namely Unsupervised ML Reconnection, in Python language, in the context of the EU AIDA project. We share here the links to the new version of the scripts where the small bug has been corrected: https://gitlab.com/aidaspace/aidapy/-/tree/unsuperv_rec_2/aidapy/unsupmr and, for Zenodo, https://doi.org/10.5281/zenodo.5118596 (version 2.0.0). We also take advantage of this opportunity to signal a misspelling: "Davis–Bouldin index" should be "Davies–Bouldin index."

Table 3
Number of Structures Found, Precision and nMR-precision for AML, for Different AR Thresholds (from 10 to 70)

Time $[1/\Omega_{ci}]$		20	230	247	282	494	Mean ($3t$)	Mean ($4t$)
N. structures		35	29	19	24	32		
N. structures	AR > 10	0	20	17	22	30		
	AR > 12.5	0	18	17	21	30		
	AR > 20	0	15	17	20	23		
	AR > 30	0	14	13	14	18		
	AR > 50	0	8	10	13	9		
	AR > 70	0	6	9	12	7		
precision	AR > 10	⋯	0.6	0.82	0.64	0.4	0.69	0.61
	AR > 12.5	⋯	0.67	0.82	0.67	0.4	0.72	0.64
	AR > 20	⋯	0.73	0.82	0.7	0.39	0.75	0.66
	AR > 30	⋯	0.79	0.85	0.79	0.39	0.81	0.70
	AR > 50	⋯	1	1	0.77	0.33	0.92	0.77
	AR > 70	⋯	1	1	0.75	0.43	0.92	0.79
nMR-precision	AR < 10	1	1	1	1	1	1	1
	AR < 12.5	1	1	1	1	1	1	1
	AR < 20	1	0.93	1	1	0.67	0.98	0.9
	AR < 30	1	0.93	0.5	0.7	0.64	0.71	0.69
	AR < 50	1	0.81	0.55	0.64	0.61	0.67	0.65
	AR < 70	1	0.74	0.5	0.58	0.64	0.61	0.61

Note. The results are shown for five different times of our simulation: $t \sim 20[1/\Omega_{ci}]$, $t \sim 230[1/\Omega_{ci}]$, $t \sim 247[1/\Omega_{ci}]$, $t \sim 282[1/\Omega_{ci}]$, and $t \sim 494[1/\Omega_{ci}]$. In the last two columns we report the mean value of our quality parameters for the three central times (230, 247, and 282) and for four times (230, 247, 282, and 494). In the second row we list the number of structures found at the end of the third step; in the third to eighth rows we give the number of detected structures overcoming the specified AR threshold. In the ninth to fourteenth rows we give the values of precision for different AR thresholds computed among the structures enumerated in the third to eighth rows; finally in the fifteenth to twentieth rows we give values for nMR-precision.

Table 4
Number of Structures Found, Precision and nMR-precision for A1, for Different AR Thresholds (from 10 to 70)

Time $[1/\Omega_{ci}]$		20	230	247	282	494	Mean ($3t$)	Mean ($4t$)
N. structures		12	46	48	52	454		
N. structures	AR >10	0	23	25	21	108		
	AR >12.5	0	23	25	18	93		
	AR >20	0	20	17	14	61		
	AR >30	0	15	15	12	39		
	AR >50	0	12	10	10	17		
	AR >70	0	11	9	7	12		
precision	AR >10	⋯	0.70	0.6	0.52	0.26	0.61	0.52
	AR >12.5	⋯	0.70	0.6	0.61	0.26	0.64	0.54
	AR >20	⋯	0.75	0.71	0.71	0.28	0.72	0.61
	AR >30	⋯	0.8	0.8	0.75	0.33	0.78	0.67
	AR >50	⋯	0.83	0.9	0.8	0.41	0.84	0.73
	AR >70	⋯	0.82	1	0.86	0.42	0.89	0.77
nMR-precision	AR <10	1	0.74	0.78	0.61	0.91	0.71	0.76
	AR <12.5	1	0.74	0.78	0.65	0.90	0.72	0.77
	AR <20	1	0.73	0.74	0.66	0.89	0.71	0.75
	AR <30	1	0.68	0.76	0.65	0.89	0.70	0.74
	AR <50	1	0.65	0.71	0.64	0.88	0.67	0.72
	AR <70	1	0.63	0.72	0.62	0.88	0.65	0.71

Note. The results are shown for five different times of our simulation: $t \sim 20[1/\Omega_{ci}]$, $t \sim 230[1/\Omega_{ci}]$, $t \sim 247[1/\Omega_{ci}]$, $t \sim 282[1/\Omega_{ci}]$, and $t \sim 494[1/\Omega_{ci}]$. In the last two columns we report the mean value of our quality parameters for the three central times (230, 247, and 282) and for four times (230, 247, 282, and 494). In the second row we list the number of structures found at the end of the third step; in the third to eighth rows we give the number of detected structures overcoming the specified AR threshold. In the ninth to fourteenth rows we give the values of precision for different AR thresholds computed among the structures enumerated in the third to eighth rows; finally in the fifteenth to twentieth rows we give values for nMR-precision.

Table 5
Number of Structures Found, Precision and nMR-precision for A2, for Different AR Thresholds (from 10 to 70)

Tempo $[1/\Omega_{ci}]$		20	230	247	282	494	Mean ($3t$)	Mean ($4t$)
N. structures		2	30	27	26	126		
N. structures	AR >10	0	21	20	14	56		
	AR >12.5	0	21	15	12	54		
	AR >20	0	18	14	11	38		
	AR >30	0	15	10	10	27		
	AR >50	0	12	9	9	14		
	AR >70	0	11	6	7	9		
precision	AR >10	⋯	0.76	0.75	0.79	0.36	0.77	0.66
	AR >12.5	⋯	0.76	0.75	0.92	0.33	0.81	0.69
	AR >20	⋯	0.83	0.8	0.91	0.34	0.85	0.72
	AR >30	⋯	0.8	0.86	0.9	0.37	0.85	0.73
	AR >50	⋯	0.83	0.9	0.89	0.43	0.87	0.76
	AR >70	⋯	0.81	1	0.86	0.44	0.89	0.78
nMR-precision	AR <10	1	0.89	0.43	0.58	0.84	0.62	0.68
	AR <12.5	1	0.89	0.43	0.64	0.82	0.65	0.69
	AR <20	1	0.83	0.42	0.6	0.79	0.62	0.66
	AR <30	1	0.67	0.46	0.56	0.79	0.56	0.62
	AR <50	1	0.61	0.41	0.53	0.78	0.52	0.58
	AR <70	1	0.58	0.44	0.47	0.77	0.50	0.56

Note. The results are shown for five different times of our simulation: $t \sim 20[1/\Omega_{ci}]$, $t \sim 230[1/\Omega_{ci}]$, $t \sim 247[1/\Omega_{ci}]$, $t \sim 282[1/\Omega_{ci}]$, and $t \sim 494[1/\Omega_{ci}]$. In the last two columns we report the mean value of our quality parameters for the three central times (230, 247, and 282) and for four times (230, 247, 282, and 494). In the second row we list the number of structures found at the end of the third step; in the third to eighth rows we give the number of detected structures overcoming the specified AR threshold. In the ninth to fourteenth rows we give the values of precision for different AR thresholds computed among the structures enumerated in the third to eighth rows; finally in the fifteenth to twentieth rows we give values for nMR-precision.

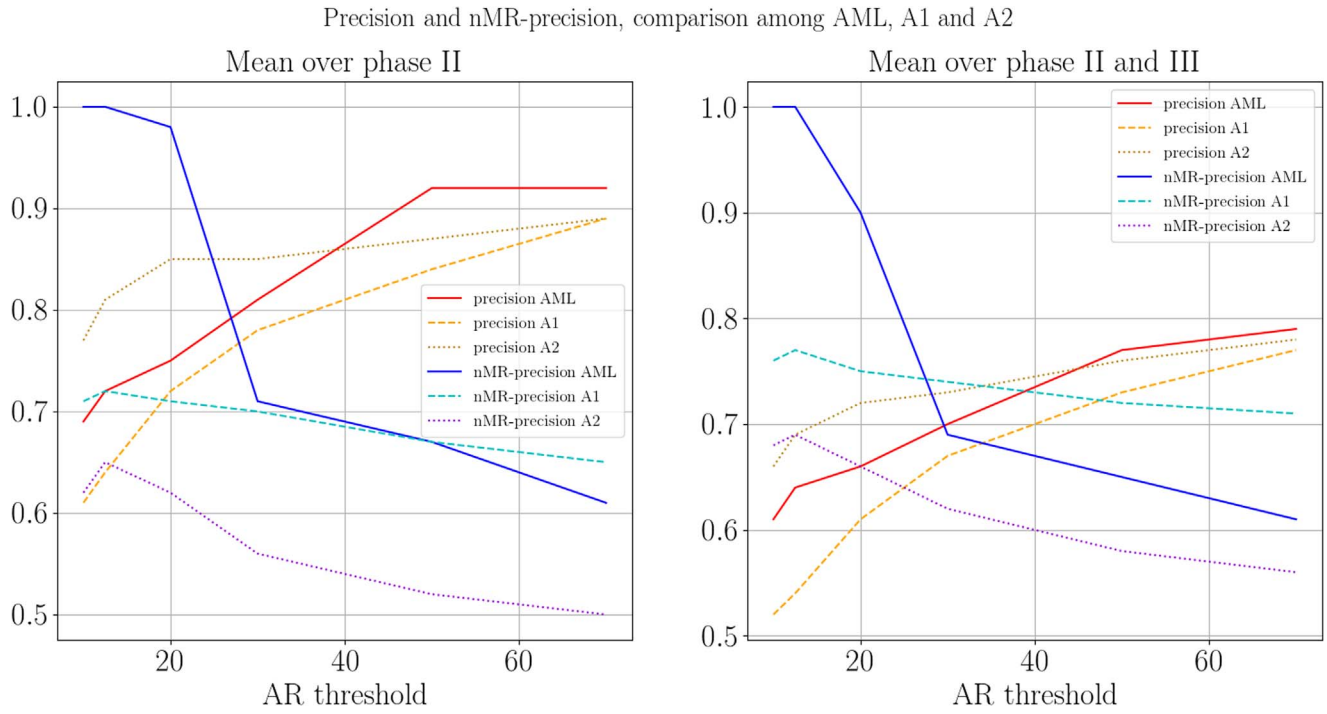


Figure 6. Plots of the values of precision (red, orange, and brown lines) and nMR-precision (blue, cyan, and violet lines) averaged over the three central times (left panel) and over four times (right panel), as a function of the AR threshold, for the three different methods we are analyzing: solid line, AML; dashed line, A1; dotted line, A2.

ORCID iDs

Manuela Sisti https://orcid.org/0000-0003-3331-0606
Matteo Faganello https://orcid.org/0000-0002-5232-0108
Francesco Califano https://orcid.org/0000-0002-9626-4371